ENVIRONMENTAL RESEARCH
LETTERS

ACCEPTED MANUSCRIPT • OPEN ACCESS

A brown wave of riparian woodland mortality following groundwater declines during the 2012-2019 California drought

To cite this article before publication: Christopher L. Kibler *et al* 2021 *Environ. Res. Lett.* in press https://doi.org/10.1088/1748-9326/ac1377

A brown wave of riparian woodland mortality following groundwater declines during the 2012-2019 California drought

Christopher L. Kibler [a], E. Claire Schmidt [b], Dar A. Roberts [ac], John C. Stella [d], Li Kui [ce], Adam M. Lambert [ef], Michael Bliss Singer [cgh]

[a] Department of Geography, University of California, Santa Barbara, CA 93106

[b] Department of Biology, Knox College, Galesburg, IL 61401

[c] Earth Research Institute, University of California, Santa Barbara, CA 93106

[d] Department of Sustainable Resources Management, State University of New York College of Environmental Science and Forestry, Syracuse, NY 13210

[e] Marine Science Institute, University of California, Santa Barbara, CA 93106

[f] Cheadle Center for Biodiversity and Ecological Restoration, University of California, Santa Barbara, CA 93106

[g] School of Earth and Environmental Sciences, Cardiff University, Cardiff, CF10 3AT, United Kingdom

[h] Water Research Institute, Cardiff University, Cardiff, CF10 3AT, United Kingdom

Abstract

As droughts become more frequent and more severe under anthropogenic climate change, water stress due to diminished subsurface supplies may threaten the health and function of semi-arid riparian woodlands, which are assumed to be largely groundwater dependent. To better support the management of riparian woodlands under changing climatic conditions, it is essential to understand the sensitivity of riparian woodlands to depth to groundwater (DTG) across space and time. In this study, we examined six stands of riparian woodland along 28 km of the Santa Clara River in southern California. Combining remote sensing data of fractional land cover, based on spectral mixture analysis, with historical groundwater data, we assessed changes in riparian woodland health in response to DTG during the unprecedented 2012-2019 California

drought. We observed a coherent "brown wave" of tree mortality, characterized by decreases in healthy vegetation cover and increases in dead/woody vegetation cover, which progressed downstream through the Santa Clara River corridor between 2012 and 2016. We also found consistent, significant relationships between DTG and healthy vegetation cover, and separately between DTG and dead/woody vegetation cover, indicating that woodland health deteriorated in a predictable fashion as the water table declined at different sites and different times. Based on these findings, we conclude that the brown wave of vegetation dieback was likely caused by local changes in DTG associated with the propagation of precipitation deficits into a depleted shallow alluvial aquifer. These factors suggest that semi-arid riparian woodlands are strongly dependent on shallow groundwater availability, which is in turn sensitive to climate forcing.

1. Introduction

Riparian trees often rely on shallow groundwater to meet their water needs, so water table declines during increasingly frequent and severe drought conditions threaten the health and function of riparian woodlands (Diffenbaugh et al., 2015; Meixner et al., 2016; Rohde et al., 2017; Williams et al., 2020). Though many studies have examined the sensitivity of individual species to drought and local groundwater availability (e.g., Stromberg et al., 1996; Singer et al., 2014; Sargeant and Singer, 2016; Petit et al., 2018; Skiadaresis et al., 2021), few studies have considered the landscape-scale responses of riparian woodlands to drought across space and time, and even fewer in relation to direct groundwater measurements (but see Rohde et al., 2021). These knowledge gaps are relevant to dryland watersheds around the globe, where convergent pressures on water resources from agriculture, urban development, and climate change are increasing (Taylor et al., 2013; Rohde et al., 2017; Rateb et al., 2020).

Riparian woodlands are ecologically important plant communities that provide habitat for sensitive animal species (Kus, 1998; Merritt and Bateman, 2012; Bateman and Merritt, 2020), promote plant biodiversity (Stromberg et al., 1996; Stromberg and Merritt, 2016), and contain a disproportionately large amount of the biomass in dryland watersheds (Swetnam et al., 2017; Matzek et al., 2018; Dybala et al., 2019). They form in convergent topographic zones, which serve as hydrologic refugia and are somewhat buffered from normal climatic variability (Brooks et al., 2015; Hoylman et al., 2019). Riparian tree species are typically phreatophytes, which have taproot systems that extend up to 5 m down to the capillary fringe above perennial water tables (Stromberg, 2013; Rohde et al., 2017). Phreatophytes are extremely sensitive to water availability at all life stages (Mahoney and Rood, 1998; Stella and Battles, 2010; Singer et al., 2013). If their root systems lose contact with the alluvial water table, phreatophytes commonly exhibit stomatal closure, leaf abscission, branch dieback, and xylem cavitation (Scott et al., 1999; Leffler et al., 2000; Rood et al., 2000). Prolonged water table declines, for example during extreme drought conditions, can lead to whole-plant mortality if a tree's hydraulic system cannot maintain a favorable water balance as groundwater supply declines (Scott et al., 1999; Cooper et al., 2003).

From 2012 to 2019, California experienced the most severe drought in its paleoclimate record (Robeson et al., 2015). Meteorological drought conditions first emerged in northern California around January 2012 and then spread southward (U.S. Drought Monitor, 2021). The meteorological drought propagated into hydrological (Van Loon, 2015) and ecological (Kovach et al., 2019; Munson et al., 2020) droughts in dryland regions throughout southern California (Okin et al., 2018; Dong et al., 2019; Warter et al., 2020). Record low precipitation and record high temperatures (Diffenbaugh et al., 2015) substantially reduced soil moisture (Warter et al.,

2020), streamflow (Konrad, 2019), groundwater storage (Thomas et al., 2017), and upland canopy water content (Asner et al., 2016) throughout the region. While the drought is known to have generated mass die-off of upland trees (e.g., Goulden and Bales, 2019), there is a notable lack of quantitative assessments of drought-induced mortality of lowland riparian phreatophytes, particularly within dryland regions. Documenting large-scale ecological die-offs, particularly in ecosystems that are buffered from climate impacts by their hydrogeomorphic setting, is important for identifying global signals of forests being pushed past their tolerance for environmental change (Allen et al., 2010; Anderegg et al., 2013; Allen et al., 2015; McDowell et al., 2016).

Remote sensing is a powerful tool for analyzing the sensitivity of vegetation health to changes in the water availability, but few remote sensing studies have quantified the sensitivity of groundwater-dependent ecosystems to water table declines (e.g., Barron et al., 2014; Huntington et al., 2016). In this study, we combined time series remote sensing imagery with data from groundwater monitoring wells to investigate the fate and trajectory of riparian woodlands in southern California during the unprecedented 2012-2019 California drought. We used spectral mixture analysis to discriminate between healthy and dead vegetation cover in remote sensing imagery. We then analyzed the relationship between vegetation cover and depth to groundwater (DTG) in a range of woodland stands that represent a gradient of groundwater availability. These data enabled us to characterize the trajectory and the spatial progression of drought impacts across an ecologically and economically important river corridor, and to monitor the initial drought recovery in the riparian woodlands.

2. Methods

2.1 Study Area

The Santa Clara River flows 132 km from the Mojave Desert to the Pacific Ocean and has a catchment covering 4,200 km^2 in Ventura and Los Angeles Counties, California (Beller et al., 2016). Mean annual precipitation ranges from 200–800 mm, with the wettest regions at high elevations (catchment relief 2,700 m) and near the coast (Downs et al., 2013). The basin has a Mediterranean climate with cool, wet winters and warm, dry summers, and many reaches of the Santa Clara River are ephemeral (i.e., flowing only part of most years). Winter rainfall produces flashy flows, and more than half of the annual discharge occurs during a small number of precipitation events (Downs et al., 2013; Beller et al., 2016). The river corridor has been subject to extensive urban and agricultural development over the last century, but the main stem of the river has not been severely controlled by engineering structures, making it the largest river in southern California that is mostly free flowing (Downs et al., 2013; Beller et al., 2016).

The native riparian woodlands along the Santa Clara River are discontinuous, existing at locations where groundwater is close to the surface under normal conditions (Beller et al., 2016). The riparian woodlands are dominated by phreatophytic tree and shrub species, including *Populus fremontii*, *P. trichocarpa*, *Salix laevigata*, *S. lasiolepis*, and *S. exigua*. The roots for these species are typically concentrated in the top 2 m of the soil profile (Table 1; TNC, 2021), although phreatophytes exhibit a considerable degree of plasticity in rooting depth in response to local groundwater conditions (Shafroth et al., 2000; Rood et al., 2011).

Table 1: Rooting depths for tree and shrub species that are prevalent in riparian woodlands in the Santa Clara River floodplain.

Species	Rooting Depth (m)	Source
Populus fremontii	1.4 (max)	Shafroth et al. (2000)[a]
Populus fremontii	2.1+ (max)	Zimmerman (1969)
Populus fremontii	0.8 (max)	Rood et al. (2011)
Populus trichocarpa	0.65 (max)	Rood et al. (2011)
Salix laevigata	1+ (max)	Stover et al. (2018)
Salix exigua	0.51 (min)	USDA (2021)
Baccharis salicifolia	0.3 (min)	USDA (2021)
Baccharis salicifolia	0.6 (max)	Gary (1963); Stromberg (2013)

[a] Study that measured three-year-old saplings

2.2 Study Sites

We identified six stands of *Populus*-*Salix* riparian woodlands in the lower Santa Clara River floodplain that are thought to be supported by perennial shallow aquifers (Figure 1; Beller et al., 2016). The woodlands range in area from 7-120 ha, and they represent the most substantial woodlands that were present before the 2012-2019 drought (Beller et al., 2016). The study sites are distinguished by transitions in hydrology or river management that facilitate shallow groundwater depths. Site boundaries were manually digitized in GIS software using 2012 aerial imagery acquired by the National Agricultural Imagery Program (USDA, 2012).

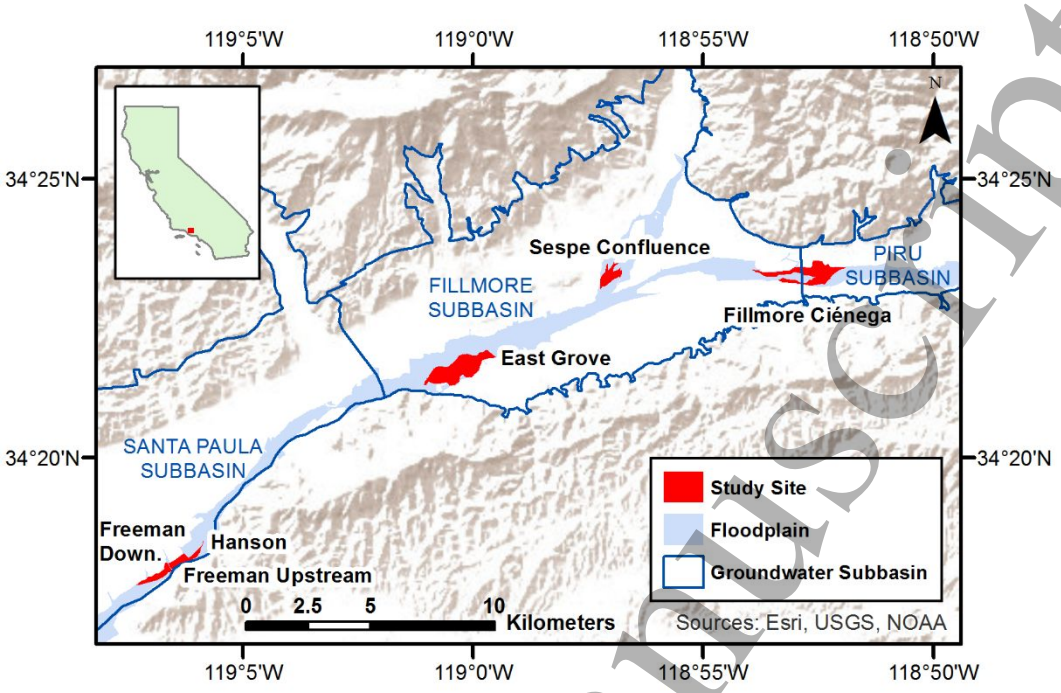

Figure 1. Location of the study sites in the floodplain of the Santa Clara River, California, USA. The river flows from east to west.

2.3 Depth to Groundwater

We calculated DTG at each of the study sites using measurements from nearby wells acquired from the California Department of Water Resources (https://sgma.water.ca.gov/webgis/?appid=SGMADataViewer), United Water Conservation District, and the County of Ventura. We also used unpublished data from shallow monitoring wells that were installed by members of our team at two of the study sites (Tables S1-S2; Figures S1-S4). The shallow wells are ~3 m deep and were installed between 2015 and 2020. They are manually measured twice per month. We used two different protocols to calculate DTG at the study sites, depending on the well data availability for each site (see supplementary material).

2.4 Remote Sensing Data Acquisition and Processing

Spectral mixture analysis (SMA) was used to map the fractional cover of green vegetation (GV), non-photosynthetic vegetation (NPV; i.e., dead and woody plant material), and

soil in the Santa Clara River floodplain (Smith et al., 1990; Roberts et al., 1998). The SMA model was calibrated using data from the Airborne Visible/Infrared Imaging Spectrometer (Green et al., 1998) and *in situ* spectra (see supplementary material). We analyzed Landsat images (spatial resolution of 30 m) acquired every June between 2011 and 2018. The June 2011 image provides a pre-drought baseline (U.S. Drought Monitor, 2021). The June 2012-2018 images capture all of the growing seasons during the drought. Data from 2012 were omitted because of the scan line corrector failure on Landsat 7 (Markham et al., 2004). The SMA model generated estimates of the fractional cover of GV, NPV, and soil within each pixel for each image. While the SMA method did not classify species cover, qualitative observations of species cover were made during field visits to the sites between 2017 and 2021, and by manually examining high resolution aerial imagery captured before, during, and after the drought.

2.5 Analysis of Drought Effects on Vegetation

The fractional cover data and the groundwater data were used to conduct two analyses. First, the GV and NPV fractions were used to examine the spatial and temporal trends of woodland mortality along the river corridor. Mortality was indicated by a decrease in GV fractions and an increase in NPV fractions (Huang et al., 2019). Significant differences in land cover fractions for each study site across time were identified using a Kruskal-Wallis test and a post-hoc Dunn's test with a Holm adjustment ($\alpha = 0.05$).

Second, we quantified the sensitivity of GV and NPV fractions to DTG. The median GV and NPV fractions were calculated for each study site and each year. We used the DTG measurements that were closest in time to the Landsat image acquisition dates. The difference between the well measurement dates and the image acquisition dates ranged from 0 days to 36 days with a median of 13 days. The sensitivity analyses were divided into two distinct time

spans. The first time span was limited to data from 2011 to 2016, representing the period when the drought became progressively more severe, as evidenced by increasing DTG, below-average soil moisture (Warter et al., 2020), and decreasing SPEI. The 2011-2016 observations were pooled across sites and years, and mixed effect logistic-binomial regression (Gelman and Hill, 2006) was used to determine if DTG is a significant predictor of GV and NPV fractions. Site was included as a random effect in the models to account for local influences on the vegetation unrelated to groundwater (see supplementary material).

The second time span was limited to data from 2017 and 2018, which represents a period of early drought recovery in the riparian woodlands. Substantial rainfall in the winter of 2016-2017 reduced DTG and increased soil moisture in the region (Warter et al., 2020). As a result, the ecological drought began to subside, even though meteorological drought conditions persisted until 2019. The sensitivity of an ecological response to an environmental driver often differs based on the direction of the change. Differing sensitivities during decline and recovery phases can result in hysteresis in ecological systems (Beisner et al., 2003; Andersen et al., 2009). The 2017-2018 data were used to determine if there were differences in the sensitivity to DTG during the early stages of drought recovery as compared to the drought onset years of 2011-2016. The observed land cover fractions from 2017 and 2018 were compared to the values predicted by the regression model that was calibrated using data from 2011-2016. This indicated whether sensitivity to DTG differed during the two phases. Mean absolute error (MAE) was used to quantify the difference between the observed and predicted values during the two phases.

3. Results

3.1 Drought Timeline

The Santa Clara River watershed experienced moderate drought conditions throughout much of 2012 and consistently experienced severe drought conditions starting in June 2013 (Figure 2; U.S. Drought Monitor, 2021). Rainfall in the winter of 2016-2017 provided some drought relief, but severe drought conditions returned in 2018 (U.S. Drought Monitor, 2021). Persistent rainfall from a series of atmospheric rivers (Sumargo et al., 2021) ended the drought in the winter of 2018-2019. Standardized Precipitation Evaporation Index (Vincente-Serrano et al., 2010) values generally remained positive after February 2019, and the U.S. Drought Monitor, a composite drought index, also indicated that the drought ended in February 2019.

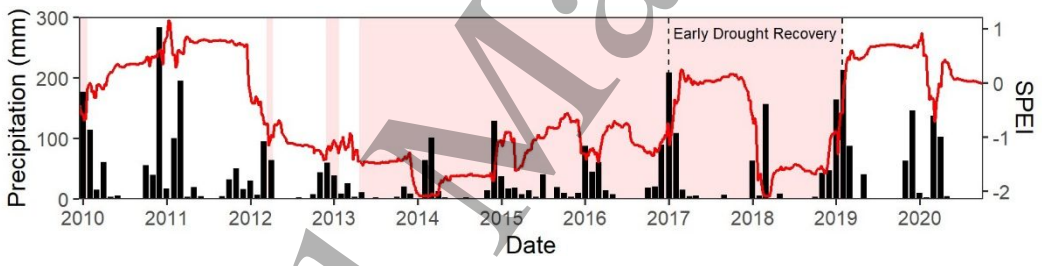

Figure 2. Mean monthly precipitation (black bars) and 12-month Standardized Precipitation Evaporation Index (SPEI; red line) in the Santa Clara River watershed (Abatzoglou, 2013; Huntington et al., 2017). The red shading indicates periods of drought according to the U.S. Drought Monitor (2021). The date labels indicate January 1 of each year.

3.2 Groundwater Level Changes During and After Drought

In 2011, maximum DTG at the six study sites ranged from 1.1 to 4.4 m. The DTG increased (i.e., the water table declined) at all six study sites between 2011 and 2016, but there was substantial spatial and temporal variability in DTG along the river corridor (Figure 3; Table S3). The changes in DTG were mediated by the interaction between climatic forcings and basin geomorphology. The Fillmore Ciénega site sits at the boundary of the Piru and Filmore groundwater subbasins (Figure 1), where the deposits of permeable alluvium become

substantially narrower and shallower and force groundwater to the surface (Mann, 1958; Reichard et al., 1999). Surface flow between the Piru and Fillmore subbasins decreased between 2011 and 2013 and stopped between 2014 and 2016 (UWCD, 2017). As a result, shallow lateral recharge of the Fillmore subbasin was likely reduced or eliminated during the peak of the drought. Maximum DTG at Fillmore Ciénega and Sespe Confluence increased by 11.9 m and 12.7 m, respectively, between 2011 and 2016 as groundwater in the Fillmore subbasin was depleted. At the downstream end of the Fillmore subbasin, groundwater elevations were more stable. The East Grove site sits at the boundary of the Fillmore and Santa Paula subbasins, where constrictions in the deposits of unconsolidated alluvium again force groundwater to the surface (Reichard et al., 1999). Maximum DTG at the East Grove site only increased by 0.9 m between 2011 and 2016. Surface flow at the boundary between the Fillmore and Santa Paula subbasins did not approach zero until 2016 (UWCD, 2017). The Hanson, Freeman Upstream, and Freeman Downstream sites are located in the Santa Paula subbasin, where the shallow aquifer sits on top of impermeable deposits that prevent groundwater from percolating into deeper aquifers (Reichard et al., 1999; Hanson et al., 2003). Groundwater elevations in the Santa Paula subbasin remained relatively stable throughout the drought. At Hanson, Freeman Upstream, and Freeman Downstream, maximum DTG increased by 3.5 m, 3.0 m, and 5.0 m (respectively) between 2011 and 2016. In 2016, maximum DTG at the six sites ranged from 2.0 to 17.1 m. Substantial rainfall in the winter of 2016-2017 reversed groundwater trends and caused DTG to decrease (i.e., the water table rose) at all study sites, but some sites did not approach pre-drought DTG until 2019.

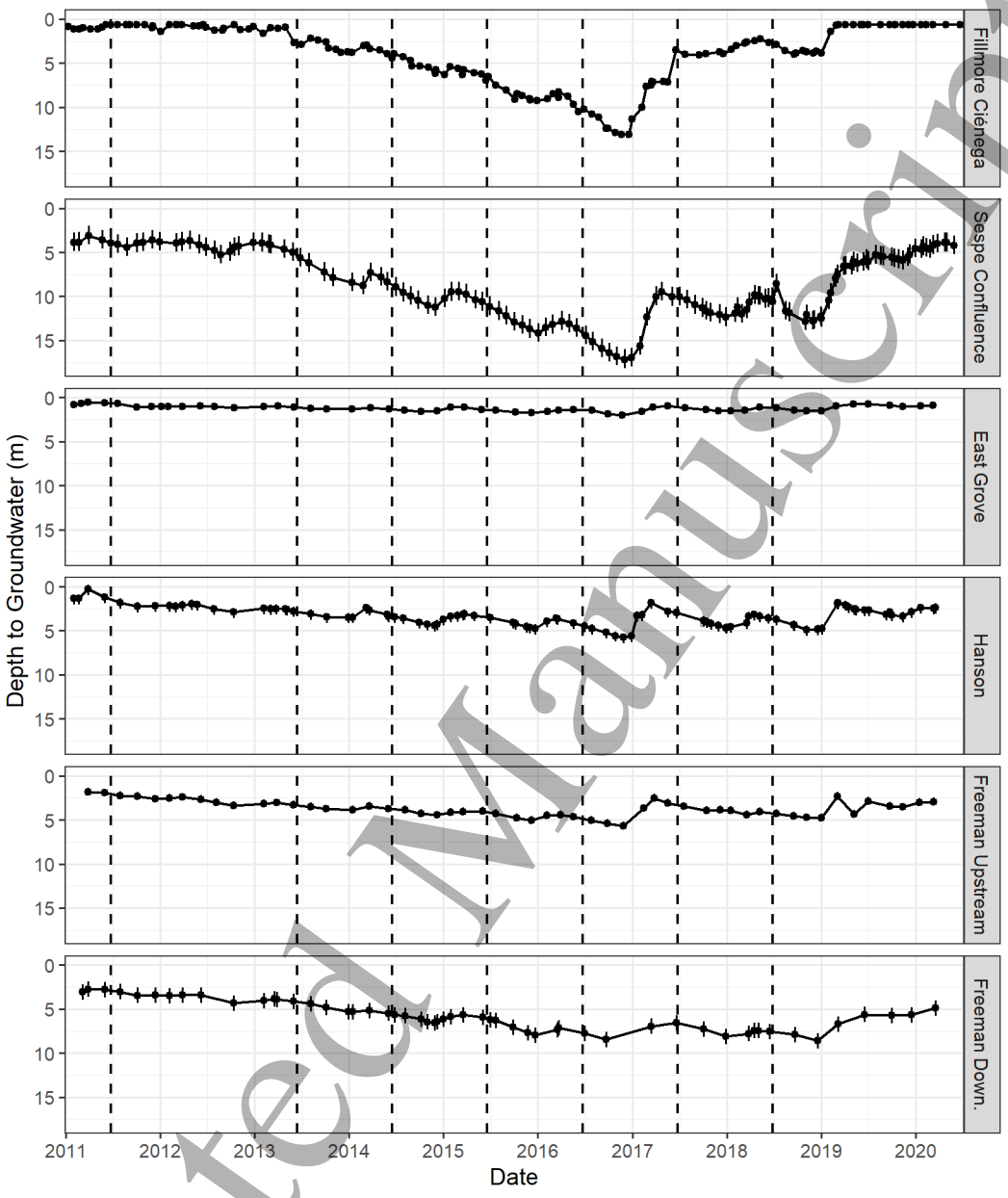

Figure 3. Mean DTG from 2011 to 2020 for each study site. The vertical bars represent the interquartile range of DTG for sites where DTG was measured by a single shallow well (see supplementary material). The dashed vertical lines indicate the remote sensing image acquisition dates. The date labels indicate January 1 of each year.

3.3 Vegetation Cover Change During Drought

Several riparian woodlands exhibited large decreases in GV cover and large increases in NPV cover from 2011 to 2016, indicating widespread drought-induced mortality (Figure 4,

Tables S4-S6). Fillmore Ciénega and Sespe Confluence exhibited the largest decreases in GV fractions and the largest increases in NPV fractions. Sites farther downstream were less affected by the drought and experienced smaller changes in land cover.

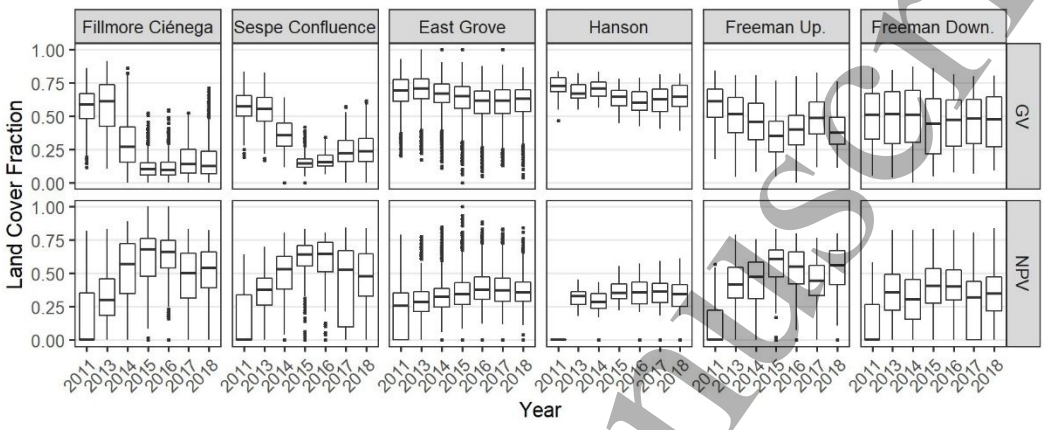

Figure 4. Box plots of green vegetation (GV) fractions and non-photosynthetic vegetation (NPV) fractions for each study site from 2011 to 2018. Note that 2012 data are omitted (see text).

There was a distinct spatial pattern and temporal trend of woodland mortality that occurred both within and across study sites in the Fillmore subbasin (Figure 5). Widespread mortality first occurred in 2013 at the most upstream study site, Fillmore Ciénega (Figure S5). A wave of mortality then traveled 13 km west (downstream) across the Fillmore subbasin between 2013 and 2016. The wave of mortality can be seen within and across individual study sites, and it is especially distinct within the Fillmore Ciénega site. By 2015, the wave of mortality reached the area immediately upstream of the East Grove site (Figure S6). By 2016, all three areas had experienced widespread mortality, and the Fillmore Ciénega and Sespe Confluence sites experienced near-complete mortality of their riparian woodlands. Sites in the downstream Santa Paula subbasin were relatively stable throughout the drought, and no distinct spatial pattern of woodland mortality in the Santa Paula subbasin was observed (Figure S7).

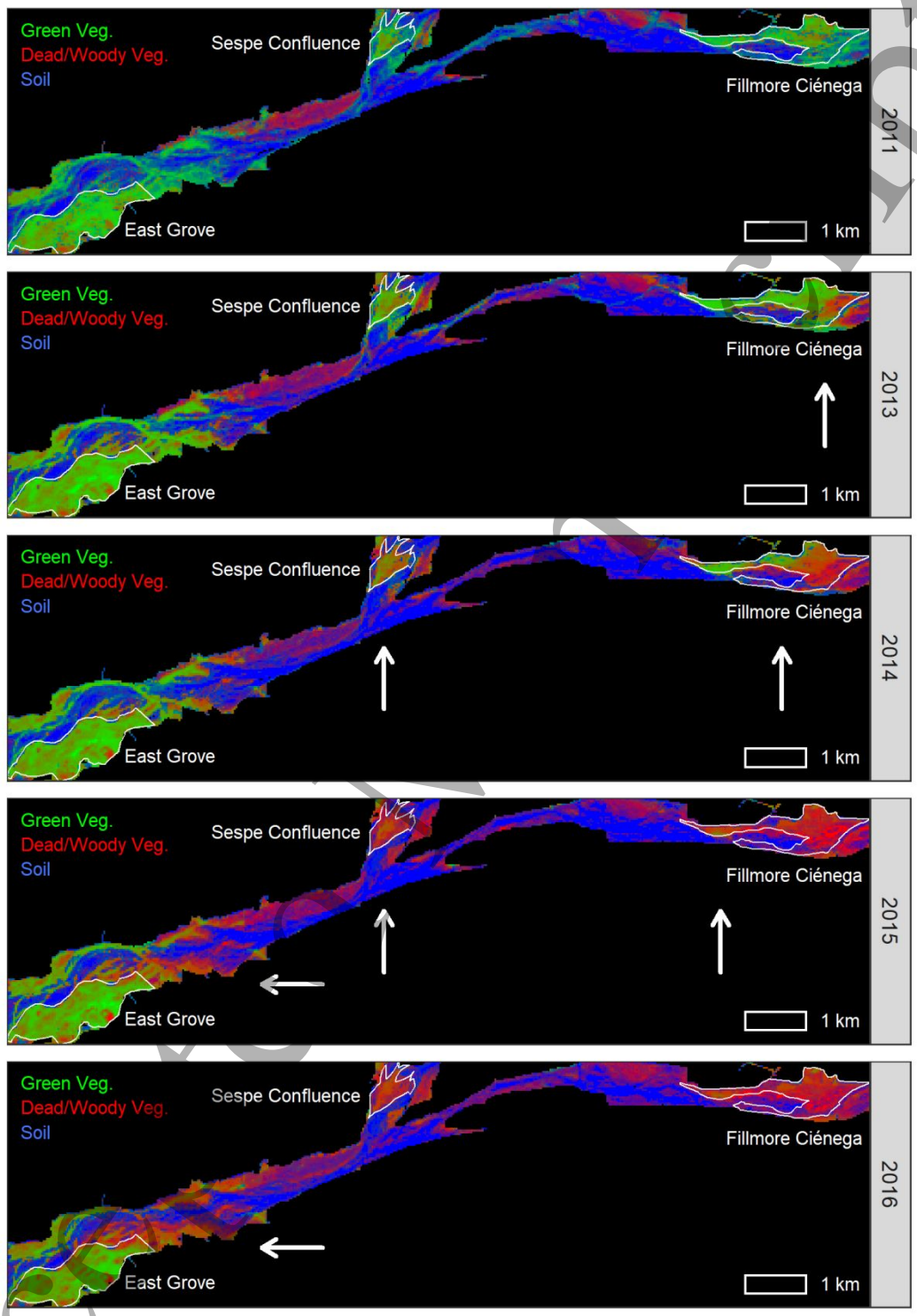

Figure 5. Remote sensing model outputs of floodplain land cover in the Fillmore subbasin from 2011 to 2016. The study sites are outlined in white, and the white arrows indicate areas experiencing notable dieback in particular years. The river flows from right to left. A comparable figure for the Hanson, Freeman Upstream, and Freeman Downstream sites is included in the supplementary material (Figure S7).

3.4 Groundwater Declines and Plant Health

DTG was significant predictor of the GV and NPV fractions for 2011-2016 (Table 2). There was a significant negative relationship between DTG and the GV fractions ($p < 0.001$; Figure 6a), indicating that green vegetation decreased as the water table declined. There was also a significant positive relationship between DTG and the NPV fractions ($p < 0.001$; Figure 6b), indicating that dead and woody plant cover increased as the water table declined. Taken together, these remote sensing metrics indicate leaf shedding, increased litter, exposed branches, and, in some cases, complete mortality as the drought progressed (Adams et al., 1995).

Table 2: Mixed effect logistic-binomial regression results for models assessing the relationship between DTG and GV fractions and between DTG and NPV fractions from 2011 to 2016. Site was included as a random effect in the models. The values in parentheses indicate the standard errors of the regression coefficients.

	GV	NPV
FIXED EFFECTS		
Intercept	1.02 ***	-2.09 ***
	(0.16)	(0.28)
DTG	-0.24 ***	0.33 ***
	(0.01)	(0.01)
RANDOM EFFECTS		
	Std. Dev	Std. Dev
Site (Intercept)	0.38	0.68
MODEL		
N	30	30
N (site)	6	6
Pseudo-R^2 (fixed)	0.16	0.24
Pseudo-R^2 (total)	0.19	0.33

*** $p < 0.001$

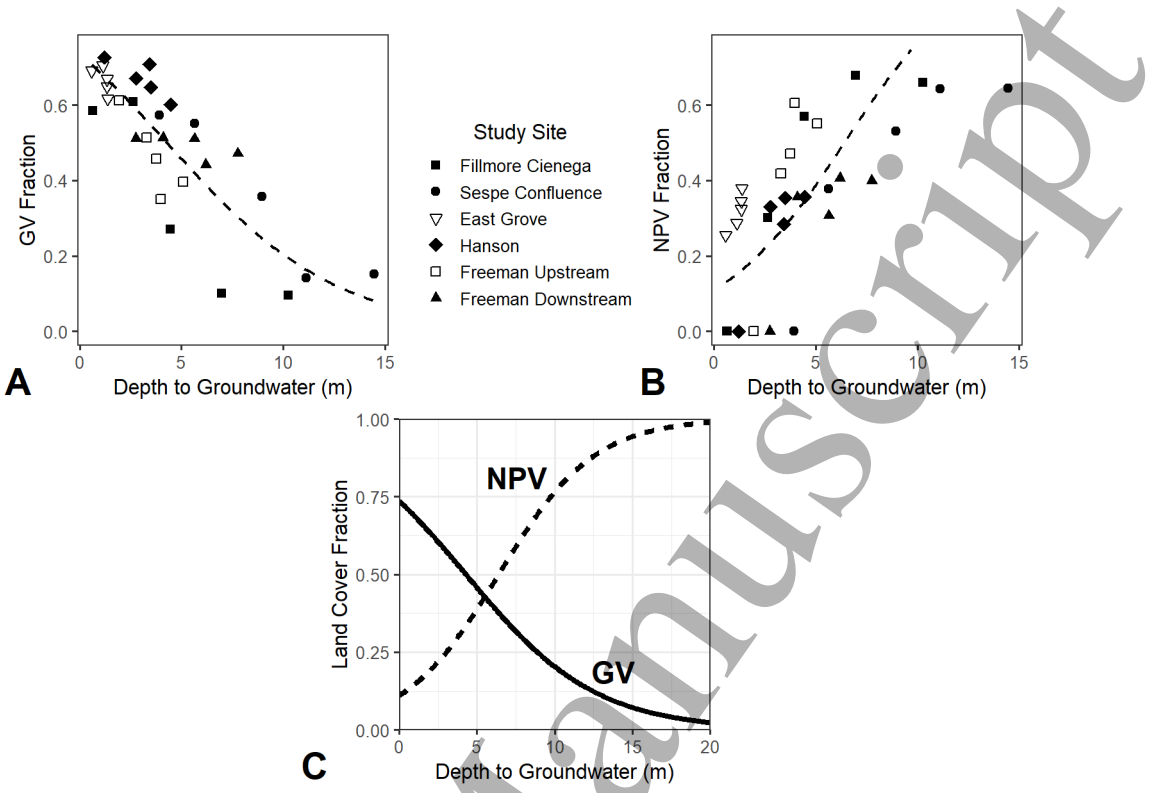

Figure 6. Scatterplots of mean DTG and median GV fractions (a) or median NPV fractions (b) from 2011 to 2016. The lines represent the modeled fixed effect of DTG on GV fractions (a,c) and NPV fractions (b,c).

3.5 Site-based Differences in Early Drought Recovery

We also compared the 2017-2018 GV fractions to the values that were predicted by the regression model, which was calibrated using data from 2011-2016. This revealed whether the sensitivity to DTG differed during the decline and recovery phases. The 2017-2018 GV fractions for Fillmore Ciénega deviated substantially from the values predicted by the model (decline MAE = 0.08; recovery MAE = 0.28). Fillmore Ciénega demonstrated a clear hysteresis signal, whereby groundwater rose by over 7 m (i.e., a reduced DTG), but there was only a modest increase in GV fractions (Figure 7). The lack of response to rising groundwater can be explained by dead vegetation covering the site. The DTG at Sespe Confluence remained relatively deep in 2017 and 2018, and the GV fractions did not deviate substantially from the values predicted by

the model (decline MAE = 0.05; recovery MAE = 0.02). The modest increase in GV fractions is likely due to the invasion of *Arundo donax* after the widespread mortality of native phreatophytes, which is a common consequence of drought conditions affecting native plants (e.g., Merritt and Poff, 2010). Field observations indicate that *A. donax* now dominates the site (Figure S8). The other sites, where the native woodlands remained largely intact (e.g., Figure S9), exhibited consistent sensitivity to DTG during the decline (MAE = 0.02-0.07) and recovery (MAE = 0.03-0.09) phases.

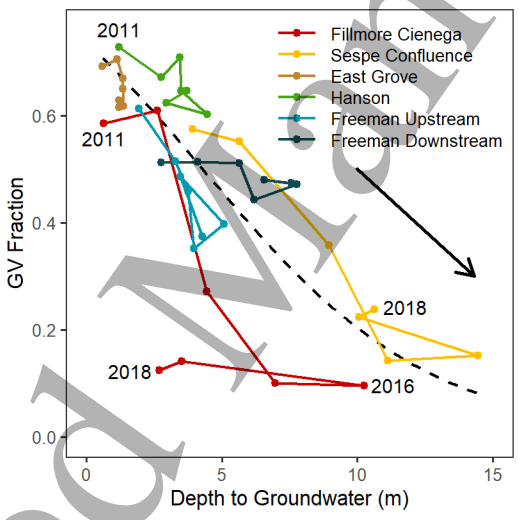

Figure 7. Scatterplot of DTG and median GV fractions from 2011 to 2018. The line segments connect observations from consecutive years. The observations from 2011 are generally in the upper left and the observations from 2018 are generally in the lower right. Observations from 2012 are omitted (see text). The dashed line represents the modeled fixed effect of DTG on GV fractions for data from 2011-2016.

4. Discussion

During the 2012-2019 California drought, riparian woodland mortality in the Santa Clara River floodplain followed a coherent spatial pattern and temporal trend that occurred across the river corridor and mirrored the apparent trend in DTG. Mortality first occurred at the upstream side of the Fillmore Ciénega site as flow between the Piru and Fillmore subbasins decreased

around 2013. A distinct "brown wave" of mortality then traveled west (i.e., upstream to downstream) between 2013 and 2016 as groundwater in the Fillmore subbasin was progressively depleted. The brown wave stopped just upstream of the East Grove site, where groundwater elevations were relatively stable and surface flow was maintained throughout most of the drought (UWCD, 2017). The brown wave reveals that riparian phreatophytes are extremely sensitive to DTG over both space and time, and that localized DTG trends play an important role in determining the fate of riparian woodlands during extreme drought conditions. Few studies have quantified the sensitivity of groundwater-dependent ecosystems to DTG (e.g., Lite and Stromberg, 2005), and only recently has it become possible to conduct spatially and temporally extensive analyses at a corridor scale (e.g., Huntington et al., 2016). Such analyses were historically limited by the available remote sensing data, which were too expensive (e.g., Zhu et al., 2019) or too coarse to resolve narrow stands of riparian woodlands (Dufour et al., 2012). Likewise, groundwater records have only recently been aggregated and made available in comprehensive data sets.

Groundwater serves as a crucial link in the chain of drought propagation from meteorological drying to plant responses by riparian phreatophytes. The 2012-2019 California drought was caused by record low precipitation and record high temperatures, which reduced water inputs to ecosystems and increased evaporative demand (Diffenbaugh et al., 2015; Warter et al., 2020). The drought generally reduced groundwater recharge (Harlow and Hagedorn, 2018) and caused groundwater elevations to decline, but subsurface water fluxes are spatially variable and are mediated by several factors including agricultural water use and runoff, river regulation, soil texture, and bedrock geology. During drought conditions, the hydrological drivers of groundwater elevation interact with meteorological trends to produce distinct spatial patterns and

temporal trends of groundwater change (Jensco and McGlynn, 2011; Harlow and Hagedorn, 2018).

The spatiotemporal variability in groundwater elevation caused varying physiological responses in the riparian woodlands in the Santa Clara River floodplain. When water tables decline by several meters, the root systems of riparian trees can lose access to groundwater (Stromberg, 2013). Riparian tree species are poorly adapted to drought and can experience catastrophic xylem cavitation at relatively high (i.e., close to zero) vapor pressure deficits (Fichot et al., 2015). To mitigate and prevent this often-irreversible change, trees undergo a series of physiological changes to maintain a favorable water balance in the face of declining water supply (Rood et al., 2003). Within minutes, they can regulate stomatal conductance to limit transpirational water loss (Horton et al., 2001; Amlin and Rood, 2003; Pivovaroff et al., 2018). Leaf abscission and branch dieback, though detrimental to woody plants in the short term, can serve as long-term survival strategies that help trees reduce water demand and prevent the loss of xylem water conductance (Scott et al., 1999; Rood et al., 2000; Cooper et al., 2003). These physiological responses may not be adequate to mitigate water stress from large and sudden water table declines, which often cause hydraulic failure and whole-plant mortality (Scott et al., 1999; Lite and Stromberg, 2005; Tai et al., 2018).

The brown wave is likely an emergent property of individual plants responding to localized changes in DTG, as evidenced by the fine-scale changes in plant health and the strong statistical relationships between the land cover fractions and DTG. Few studies have examined the spatial evolution of riparian woodland responses to water table declines (but see Stromberg et al., 1996; Scott et al., 1999, 2000; Tai et al., 2018). The current understanding of phreatophyte sensitivity to DTG is largely derived from field measurements (e.g., Horton et al., 2001; Rood et

al., 2011), laboratory experiments (e.g., Leffler et al., 2000; Stella et al., 2010), and models based on phreatophyte physiology (e.g., Tai et al., 2018). These data have resulted in a conceptual model that suggests that there is a highly non-linear relationship between DTG and plant health, whereby plant health degrades rapidly when DTG increases beyond some critical threshold (e.g., Shafroth et al., 2000; Horton et al., 2001; Lite and Stromberg, 2005). In contrast with previous studies, our observations indicate that there is a mostly linear relationship between DTG and plant health at a stand scale when DTG is less than 10 m (i.e., Figure 6c). The difference in the shape of the observed relationships may indicate a scale dependence of the analysis. While many field and laboratory-based studies examine individual plants belonging to selected species, remote sensing data detects many plants belonging to many species within a pixel (Kibler et al., 2019). The observed plants that compose riparian woodlands likely have varying structures, life histories, and tolerances for groundwater decline (Stromberg et al., 1996; Stromberg and Merritt, 2016). Nonetheless, the observed sensitivity to absolute DTG and DTG change (Table S3) were generally consistent with previously reported values. At Fillmore Ciénega and Sespe Confluence, vegetation cover stopped changing as a function of DTG between 2015 and 2016, which may indicate a fundamental limit beyond which phreatophytes experience complete mortality and the health of the surviving non-phreatophytic vegetation becomes decoupled from DTG. The recovery of phreatophytes at these sites depends on the water table returning to shallow depths and seed sources for the germination of new seedlings (Stella et al., 2006).

5. Conclusion

The statistical analyses presented here provide some of the first robust estimates of the sensitivity of riparian woodlands to DTG. Our findings also reveal that DTG trends can be highly

variable during extreme drought conditions, even within the same river corridor, which can result in distinct spatial patterns and temporal trends of plant mortality in riparian woodlands. Quantifying the sensitivity of riparian ecosystems to groundwater change will become increasingly important as anthropogenic climate change increases the frequency and severity of drought conditions across the western United States (Diffenbaugh et al., 2015; Rohde et al., 2017; Williams et al., 2020). The widespread mortality observed during the brown wave mirrors the dynamics of mass die-offs that have occurred in upland forest ecosystems (e.g., Allen et al., 2010; Goulden and Bales, 2019). Anthropogenic climate change, shifts in water availability, and other environmental forcings are overwhelming the resiliency of ecosystems that are typically buffered from climatic variability (Allen et al., 2015). Quantifying the sensitivity of both upland and lowland forests to hydroclimatic change will improve our ability to predict critical shifts in ecosystem structure and function in the coming decades.

Acknowledgements

The authors thank Jared Williams, Sean Carey, Margot Mason, Peter Downs, and David Miller for their assistance with this study. We also thank the Nature Conservancy for providing access to their properties. Support for this work came from the U.S. National Science Foundation (BCS-1660490, EAR-1700555, and EAR-1700517) and the U.S. Department of Defense's Strategic Environmental Research and Development Program (RC18-1006).

Bibliography

Abatzoglou, J. T. (2013). Development of gridded surface meteorological data for ecological applications and modelling. *International Journal of Climatology*, *33*(1), 121–131. https://doi.org/10.1002/joc.3413

Adams, J. B., Sabol, D. E., Kapos, V., Filho, R. A., Roberts, D. A., Smith, M. O., & Gillespie, A. R. (1995). Classification of multispectral images based on fractions of endmembers: Application to land-cover change in the Brazilian Amazon. *Remote Sensing of Environment*, *52*(2), 137–154. https://doi.org/10.1016/0034-4257(94)00098-8

Allen, C. D., Breshears, D. D., & McDowell, N. G. (2015). On underestimation of global vulnerability to tree mortality and forest die-off from hotter drought in the Anthropocene. *Ecosphere*, *6*(8), art129. https://doi.org/10.1890/ES15-00203.1

Allen, C. D., Macalady, A. K., Chenchouni, H., Bachelet, D., McDowell, N., Vennetier, M., Kitzberger, T., Rigling, A., Breshears, D. D., Hogg, E. H. (Ted), Gonzalez, P., Fensham, R., Zhang, Z., Castro, J., Demidova, N., Lim, J.-H., Allard, G., Running, S. W., Semerci, A., & Cobb, N. (2010). A global overview of drought and heat-induced tree mortality reveals emerging climate change risks for forests. *Forest Ecology and Management*, *259*(4), 660–684. https://doi.org/10.1016/j.foreco.2009.09.001

Amlin, N. M., & Rood, S. B. (2003). Drought stress and recovery of riparian cottonwoods due to water table alteration along Willow Creek, Alberta. *Trees*, *17*(4), 351–358. https://doi.org/10.1007/s00468-003-0245-3

Anderegg, W. R. L., Kane, J. M., & Anderegg, L. D. L. (2013). Consequences of widespread tree mortality triggered by drought and temperature stress. *Nature Climate Change*, *3*(1), 30–36. https://doi.org/10.1038/nclimate1635

Andersen, T., Carstensen, J., Hernández-García, E., & Duarte, C. M. (2009). Ecological thresholds and regime shifts: Approaches to identification. *Trends in Ecology & Evolution*, *24*(1), 49–57. https://doi.org/10.1016/j.tree.2008.07.014

Asner, G. P., Brodrick, P. G., Anderson, C. B., Vaughn, N., Knapp, D. E., & Martin, R. E. (2016). Progressive forest canopy water loss during the 2012–2015 California drought. *Proceedings of the National Academy of Sciences*, *113*(2), E249–E255. https://doi.org/10.1073/pnas.1523397113

Barron, O. V., Emelyanova, I., Van Niel, T. G., Pollock, D., & Hodgson, G. (2014). Mapping groundwater-dependent ecosystems using remote sensing measures of vegetation and moisture dynamics. *Hydrological Processes*, *28*(2), 372–385. https://doi.org/10.1002/hyp.9609

Bateman, H. L., & Merritt, D. M. (2020). Complex riparian habitats predict reptile and amphibian diversity. *Global Ecology and Conservation*, *22*, e00957. https://doi.org/10.1016/j.gecco.2020.e00957

Beisner, B., Haydon, D., & Cuddington, K. (2003). Alternative stable states in ecology. *Frontiers in Ecology and the Environment*, *1*(7), 376–382. https://doi.org/10.1890/1540-9295(2003)001[0376:ASSIE]2.0.CO;2

Beller, E. E., Downs, P. W., Grossinger, R. M., Orr, B. K., & Salomon, M. N. (2016). From past patterns to future potential: Using historical ecology to inform river restoration on an intermittent California river. *Landscape Ecology*, *31*(3), 581–600. https://doi.org/10.1007/s10980-015-0264-7

Brooks, P. D., Chorover, J., Fan, Y., Godsey, S. E., Maxwell, R. M., McNamara, J. P., & Tague, C. (2015). Hydrological partitioning in the critical zone: Recent advances and opportunities for developing transferable understanding of water cycle dynamics. *Water Resources Research*, *51*(9), 6973–6987. https://doi.org/10.1002/2015WR017039

Choat, B., Brodribb, T. J., Brodersen, C. R., Duursma, R. A., López, R., & Medlyn, B. E. (2018). Triggers of tree mortality under drought. *Nature*, *558*(7711), 531–539. https://doi.org/10.1038/s41586-018-0240-x

Cooper, D. J., D'Amico, D. R., & Scott, M. L. (2003). Physiological and morphological response patterns of *Populus deltoides* to alluvial groundwater pumping. *Environmental Management*, *31*(2), 215–226. https://doi.org/10.1007/s00267-002-2808-2

Diffenbaugh, N. S., Swain, D. L., & Touma, D. (2015). Anthropogenic warming has increased drought risk in California. *Proceedings of the National Academy of Sciences*, *112*(13), 3931–3936. https://doi.org/10.1073/pnas.1422385112

Dong, C., MacDonald, G. M., Willis, K., Gillespie, T. W., Okin, G. S., & Williams, A. P. (2019). Vegetation responses to 2012–2016 drought in northern and southern California. *Geophysical Research Letters*, *46*(7), 3810–3821. https://doi.org/10.1029/2019GL082137

Downs, P. W., Dusterhoff, S. R., & Sears, W. A. (2013). Reach-scale channel sensitivity to multiple human activities and natural events: Lower Santa Clara River, California, USA. *Geomorphology*, *189*, 121–134. https://doi.org/10.1016/j.geomorph.2013.01.023

Dufour, S., Muller, E., Straatsma, M., & Corgne, S. (2012). Image utilisation for the study and management of riparian vegetation: Overview and applications. In P. Carbonneau & H. Piégay (Eds.), *Fluvial remote sensing for science and management*. Wiley-Blackwell.

Dybala, K. E., Matzek, V., Gardali, T., & Seavy, N. E. (2019). Carbon sequestration in riparian forests: A global synthesis and meta-analysis. *Global Change Biology*, *25*(1), 57–67. https://doi.org/10.1111/gcb.14475

Fichot, R., Brignolas, F., Cochard, H., & Ceulemans, R. (2015). Vulnerability to drought-induced cavitation in poplars: Synthesis and future opportunities: Drought-induced cavitation in poplars: a review. *Plant, Cell & Environment*, *38*(7), 1233–1251. https://doi.org/10.1111/pce.12491

Gary, H. L. (1963). Root distribution of five-stamen tamarisk, seepwillow, and arrowweed. *Forest Science*, *9*(3), 311–314.

Gelman, A., & Hill, J. (2007). *Data analysis using regression and multilevel/hierarchical models*. Cambridge University Press.

Goulden, M. L., & Bales, R. C. (2019). California forest die-off linked to multi-year deep soil drying in 2012–2015 drought. *Nature Geoscience*, *12*(8), 632–637. https://doi.org/10.1038/s41561-019-0388-5

Green, R. O., Eastwood, M. L., Sarture, C. M., Chrien, T. G., Aronsson, M., Chippendale, B. J., Faust, J. A., Pavri, B. E., Chovit, C. J., Solis, M., Olah, M. R., & Williams, O. (1998). Imaging spectroscopy and the Airborne Visible/Infrared Imaging Spectrometer (AVIRIS). *Remote Sensing of Environment*, *65*(3), 227–248. https://doi.org/10.1016/S0034-4257(98)00064-9

Hanson, R. T., Martin, P., & Koczot, K. M. (2003). *Simulation of Ground-Water/Surface-Water Flow in the Santa Clara–Calleguas Ground-Water Basin, Ventura County, California* (Water-Resources Investigations Report No. 02–4136; p. 157). U.S. Geological Survey. https://pubs.usgs.gov/wri/wri024136/text.html

Harlow, J., & Hagedorn, B. (2018). SWB modeling of groundwater recharge on Catalina Island, California, during a period of severe drought. *Water*, *11*(1), 58. https://doi.org/10.3390/w11010058

Horton, J. L., Kolb, T. E., & Hart, S. C. (2001). Responses of riparian trees to interannual variation in ground water depth in a semi-arid river basin. *Plant, Cell and Environment*, *24*(3), 293–304. https://doi.org/10.1046/j.1365-3040.2001.00681.x

Hoylman, Z. H., Jencso, K. G., Hu, J., Holden, Z. A., Allred, B., Dobrowski, S., Robinson, N., Martin, J. T., Affleck, D., & Seielstad, C. (2019). The topographic signature of ecosystem climate sensitivity in the western United States. *Geophysical Research Letters*, *46*(24), 14508–14520. https://doi.org/10.1029/2019GL085546

Huang, C., Anderegg, W. R. L., & Asner, G. P. (2019). Remote sensing of forest die-off in the Anthropocene: From plant ecophysiology to canopy structure. *Remote Sensing of Environment*, *231*, 111233. https://doi.org/10.1016/j.rse.2019.111233

Huntington, J. L., Hegewisch, K. C., Daudert, B., Morton, C. G., Abatzoglou, J. T., McEvoy, D. J., & Erickson, T. (2017). Climate Engine: Cloud computing and visualization of climate and remote sensing data for advanced natural resource monitoring and process understanding. *Bulletin of the American Meteorological Society*, *98*(11), 2397–2410. https://doi.org/10.1175/BAMS-D-15-00324.1

Huntington, J., McGwire, K., Morton, C., Snyder, K., Peterson, S., Erickson, T., Niswonger, R., Carroll, R., Smith, G., & Allen, R. (2016). Assessing the role of climate and resource management on groundwater dependent ecosystem changes in arid environments with the Landsat archive. *Remote Sensing of Environment*, *185*, 186–197. https://doi.org/10.1016/j.rse.2016.07.004

Jencso, K. G., & McGlynn, B. L. (2011). Hierarchical controls on runoff generation: Topographically driven hydrologic connectivity, geology, and vegetation. *Water Resources Research*, *47*(11). https://doi.org/10.1029/2011WR010666

Kibler, C. L., Parkinson, A.-M. L., Peterson, S. H., Roberts, D. A., D'Antonio, C. M., Meerdink, S. K., & Sweeney, S. H. (2019). Monitoring post-fire recovery of chaparral and conifer species using field surveys and Landsat time series. *Remote Sensing*, *11*(24), 2963. https://doi.org/10.3390/rs11242963

Konrad, C. P. (2019). Seasonal precipitation influences streamflow vulnerability to the 2015 drought in the western United States. *Journal of Hydrometeorology*, *20*(7), 1261–1274. https://doi.org/10.1175/JHM-D-18-0121.1

Kovach, R. P., Dunham, J. B., Al-Chokhachy, R., Snyder, C. D., Letcher, B. H., Young, J. A., Beever, E. A., Pederson, G. T., Lynch, A. J., Hitt, N. P., Konrad, C. P., Jaeger, K. L., Rea, A. H., Sepulveda, A. J., Lambert, P. M., Stoker, J., Giersch, J. J., & Muhlfeld, C. C. (2019). An integrated framework for ecological drought across riverscapes of North America. *BioScience*, *69*(6), 418–431. https://doi.org/10.1093/biosci/biz040

Kus, B. E. (1998). Use of restored riparian habitat by the endangered Least Bell's Vireo (Vireo bellii pusillus). *Restoration Ecology*, *6*(1), 75–82. https://doi.org/10.1046/j.1526-100x.1998.06110.x

Leffler, A. J., England, L. E., & Naito, J. (2000). Vulnerability of Fremont cottonwood (Populus fremontii Wats.) individuals to xylem cavitation. *Western North American Naturalist*, *60*(2), 204–210.

Lite, S. J., & Stromberg, J. C. (2005). Surface water and ground-water thresholds for maintaining Populus–Salix forests, San Pedro River, Arizona. *Biological Conservation*, *125*(2), 153–167. https://doi.org/10.1016/j.biocon.2005.01.020

Mahoney, J. M., & Rood, S. B. (1998). Streamflow requirements for cottonwood seedling recruitment—An integrative model. *Wetlands*, *18*(4), 634–645. https://doi.org/10.1007/BF03161678

Mann Jr., J. F. (1958). *Preliminary Outline of Groundwater Conditions Near State Fish Hatchery*. Memo to United Water Conservation District.

Markham, B. L., Storey, J. C., Williams, D. L., & Irons, J. R. (2004). Landsat sensor performance: History and current status. *IEEE Transactions on Geoscience and Remote Sensing*, *42*(12), 2691–2694. https://doi.org/10.1109/TGRS.2004.840720

Matzek, V., Stella, J., & Ropion, P. (2018). Development of a carbon calculator tool for riparian forest restoration. *Applied Vegetation Science*, *21*(4), 584–594. https://doi.org/10.1111/avsc.12400

McDowell, N. G., Williams, A. P., Xu, C., Pockman, W. T., Dickman, L. T., Sevanto, S., Pangle, R., Limousin, J., Plaut, J., Mackay, D. S., Ogee, J., Domec, J. C., Allen, C. D., Fisher, R. A., Jiang, X., Muss, J. D., Breshears, D. D., Rauscher, S. A., & Koven, C. (2016). Multi-scale predictions of massive conifer mortality due to chronic temperature rise. *Nature Climate Change*, *6*(3), 295–300. https://doi.org/10.1038/nclimate2873

Meixner, T., Manning, A. H., Stonestrom, D. A., Allen, D. M., Ajami, H., Blasch, K. W., Brookfield, A. E., Castro, C. L., Clark, J. F., Gochis, D. J., Flint, A. L., Neff, K. L., Niraula, R., Rodell, M., Scanlon, B. R., Singha, K., & Walvoord, M. A. (2016). Implications of projected climate change for groundwater recharge in the western United States. *Journal of Hydrology*, *534*, 124–138. https://doi.org/10.1016/j.jhydrol.2015.12.027

Merritt, D. M., & Bateman, H. L. (2012). Linking stream flow and groundwater to avian habitat in a desert riparian system. *Ecological Applications*, *22*(7), 1973–1988. https://doi.org/10.1890/12-0303.1

Merritt, D. M., & Poff, N. L. R. (2010). Shifting dominance of riparian Populus and Tamarix along gradients of flow alteration in western North American rivers. *Ecological Applications*, *20*(1), 135–152. https://doi.org/10.1890/08-2251.1

Munson, S. M., Bradford, J. B., & Hultine, K. R. (2020). An integrative ecological drought framework to span plant stress to ecosystem transformation. *Ecosystems*. https://doi.org/10.1007/s10021-020-00555-y

Okin, G. S., Dong, C., Willis, K. S., Gillespie, T. W., & MacDonald, G. M. (2018). The impact of drought on native southern California vegetation: Remote sensing analysis using MODIS-derived time series. *Journal of Geophysical Research: Biogeosciences*, *123*(6), 1927–1939. https://doi.org/10.1029/2018JG004485

Perry, L. G., Andersen, D. C., Reynolds, L. V., Nelson, S. M., & Shafroth, P. B. (2012). Vulnerability of riparian ecosystems to elevated CO_2 and climate change in arid and semiarid western North America. *Global Change Biology*, *18*(3), 821–842. https://doi.org/10.1111/j.1365-2486.2011.02588.x

Pettit, N. E., & Froend, R. H. (2018). How important is groundwater availability and stream perenniality to riparian and floodplain tree growth? *Hydrological Processes*, *32*(10), 1502–1514. https://doi.org/10.1002/hyp.11510

Pivovaroff, A. L., Cook, V. M. W., & Santiago, L. S. (2018). Stomatal behaviour and stem xylem traits are coordinated for woody plant species under exceptional drought conditions: Xylem and stomata under extreme drought. *Plant, Cell & Environment*, *41*(11), 2617–2626. https://doi.org/10.1111/pce.13367

Rateb, A., Scanlon, B. R., Pool, D. R., Sun, A., Zhang, Z., Chen, J., Clark, B., Faunt, C. C., Haugh, C. J., Hill, M., Hobza, C., McGuire, V. L., Reitz, M., Müller Schmied, H., Sutanudjaja, E. H., Swenson, S., Wiese, D., Xia, Y., & Zell, W. (2020). Comparison of groundwater storage changes from GRACE satellites with monitoring and modeling of major U.S. aquifers. *Water Resources Research*, *56*(12). https://doi.org/10.1029/2020WR027556

Reichard, E. G., Crawford, S. M., Paybins, K. S., Martin, P., Land, M., & Nishikawa, T. (1999). *Evaluation of Surface-Water/Ground-Water Interactions in the Santa Clara River Valley, Ventura County, California* (Water-Resources Investigations Report No. 98–4208; p. 58). U.S. Geological Survey. https://pubs.er.usgs.gov/publication/wri984208

Roberts, D. A., Gardner, M., Church, R., Ustin, S., Scheer, G., & Green, R. O. (1998). Mapping chaparral in the Santa Monica Mountains using multiple endmember spectral mixture models. *Remote Sensing of Environment*, *65*(3), 267–279. https://doi.org/10.1016/S0034-4257(98)00037-6

Robeson, S. M. (2015). Revisiting the recent California drought as an extreme value. *Geophysical Research Letters*, *42*(16), 6771–6779. https://doi.org/10.1002/2015GL064593

Rohde, M. M., Froend, R., & Howard, J. (2017). A global synthesis of managing groundwater dependent ecosystems under sustainable groundwater policy. *Groundwater*, *55*(3), 293–301. https://doi.org/10.1111/gwat.12511

Rohde, M. M., Stella, J. C., Roberts, D. A., & Singer, M. B. (2021). Groundwater dependence of riparian woodlands and the disrupting effect of anthropogenically altered streamflow. *Proceedings of the National Academy of Sciences*, *118*(25), e2026453118. https://doi.org/10.1073/pnas.2026453118

Rood, S. B., Braatne, J. H., & Hughes, F. M. R. (2003). Ecophysiology of riparian cottonwoods: Stream flow dependency, water relations and restoration. *Tree Physiology*, *23*(16), 1113–1124. https://doi.org/10.1093/treephys/23.16.1113

Rood, S.B., Patiño, S., Coombs, K., & Tyree, M. T. (2000). Branch sacrifice: Cavitation-associated drought adaptation of riparian cottonwoods. *Trees*, *14*(5), 0248–0257. https://doi.org/10.1007/s004680050010

Rood, Stewart B., Bigelow, S. G., & Hall, A. A. (2011). Root architecture of riparian trees: River cut-banks provide natural hydraulic excavation, revealing that cottonwoods are facultative phreatophytes. *Trees*, *25*(5), 907–917. https://doi.org/10.1007/s00468-011-0565-7

Sargeant, C. I., & Singer, M. B. (2016). Sub-annual variability in historical water source use by Mediterranean riparian trees: Sub-Annual Riparian Tree Water Use. *Ecohydrology*, *9*(7), 1328–1345. https://doi.org/10.1002/eco.1730

Scott, M. L., Shafroth, P. B., & Auble, G. T. (1999). Responses of riparian cottonwoods to alluvial water table declines. *Environmental Management*, *23*(3), 347–358. https://doi.org/10.1007/s002679900191

Scott, M. L., Lines, G. C., & Auble, G. T. (2000). Channel incision and patterns of cottonwood stress and mortality along the Mojave River, California. *Journal of Arid Environments*, *44*(4), 399–414. https://doi.org/10.1006/jare.1999.0614

Shafroth, P. B., Stromberg, J. C., & Patten, D. T. (2000). Woody riparian vegetation response to different alluvial water table regimes. *Western North American Naturalist*, *60*(1), 66–76.

Singer, M. B., Sargeant, C. I., Piégay, H., Riquier, J., Wilson, R. J. S., & Evans, C. M. (2014). Floodplain ecohydrology: Climatic, anthropogenic, and local physical controls on

partitioning of water sources to riparian trees. *Water Resources Research*, *50*(5), 4490–4513. https://doi.org/10.1002/2014WR015581

Singer, M. B., Stella, J. C., Dufour, S., Piégay, H., Wilson, R. J. S., & Johnstone, L. (2013). Contrasting water-uptake and growth responses to drought in co-occurring riparian tree species. *Ecohydrology*, *6*(3), 402–412. https://doi.org/10.1002/eco.1283

Skiadaresis, G., Schwarz, J., Stahl, K., & Bauhus, J. (2021). Groundwater extraction reduces tree vitality, growth and xylem hydraulic capacity in Quercus robur during and after drought events. *Scientific Reports*, *11*(1), 5149. https://doi.org/10.1038/s41598-021-84322-6

Smith, M. O., Ustin, S. L., Adams, J. B., & Gillespie, A. R. (1990). Vegetation in deserts: I. A regional measure of abundance from multispectral images. *Remote Sensing of Environment*, *31*(1), 1–26. https://doi.org/10.1016/0034-4257(90)90074-V

Stella, J. C., & Battles, J. J. (2010). How do riparian woody seedlings survive seasonal drought? *Oecologia*, *164*(3), 579–590. https://doi.org/10.1007/s00442-010-1657-6

Stella, J. C., Battles, J. J., McBride, J. R., & Orr, B. K. (2010). Riparian seedling mortality from simulated water table recession, and the design of sustainable flow regimes on regulated rivers. *Restoration Ecology*, *18*, 284–294. https://doi.org/10.1111/j.1526-100X.2010.00651.x

Stella, J. C., Battles, J. J., Orr, B. K., & McBride, J. R. (2006). Synchrony of Seed Dispersal, Hydrology and Local Climate in a Semi-arid River Reach in California. *Ecosystems*, *9*(7), 1200–1214. https://doi.org/10.1007/s10021-005-0138-y

Stover, J., Keller, E., Dudley, T., & Langendoen, E. (2018). Fluvial geomorphology, root distribution, and tensile strength of the invasive Giant Reed, Arundo Donax and its role on stream bank stability in the Santa Clara River, southern California. *Geosciences*, *8*(8), 304. https://doi.org/10.3390/geosciences8080304

Stromberg, J. C., Tiller, R., & Richter, B. (1996). Effects of groundwater decline on riparian vegetation of semiarid regions: The San Pedro, Arizona. *Ecological Applications*, *6*(1), 113–131. https://doi.org/10.2307/2269558

Stromberg, J.C. (2013). Root patterns and hydrogeomorphic niches of riparian plants in the American Southwest. *Journal of Arid Environments*, *94*, 1–9. https://doi.org/10.1016/j.jaridenv.2013.02.004

Stromberg, Juliet C., & Merritt, D. M. (2016). Riparian plant guilds of ephemeral, intermittent and perennial rivers. *Freshwater Biology*, *61*(8), 1259–1275. https://doi.org/10.1111/fwb.12686

Sumargo, E., McMillan, H., Weihs, R., Ellis, C. J., Wilson, A. M., & Ralph, F. M. (2021). A soil moisture monitoring network to assess controls on runoff generation during atmospheric river events. *Hydrological Processes*, *35*(1). https://doi.org/10.1002/hyp.13998

Swetnam, T. L., Brooks, P. D., Barnard, H. R., Harpold, A. A., & Gallo, E. L. (2017). Topographically driven differences in energy and water constrain climatic control on forest carbon sequestration. *Ecosphere*, *8*(4), e01797. https://doi.org/10.1002/ecs2.1797

Tai, X., Mackay, D. S., Sperry, J. S., Brooks, P., Anderegg, W. R. L., Flanagan, L. B., Rood, S. B., & Hopkinson, C. (2018). Distributed plant hydraulic and hydrological modeling to understand the susceptibility of riparian woodland trees to drought-induced mortality. *Water Resources Research*, *54*, 4901–4915.

Taylor, R. G., Scanlon, B., Döll, P., Rodell, M., van Beek, R., Wada, Y., Longuevergne, L., Leblanc, M., Famiglietti, J. S., Edmunds, M., Konikow, L., Green, T. R., Chen, J., Taniguchi, M., Bierkens, M. F. P., MacDonald, A., Fan, Y., Maxwell, R. M., Yechieli, Y.,

… Treidel, H. (2013). Ground water and climate change. *Nature Climate Change*, *3*(4), 322–329. https://doi.org/10.1038/nclimate1744

The Nature Conservancy (2021). Groundwater Resource Hub. *Plant Rooting Depth Database*. https://groundwaterresourcehub.org/sgma-tools/gde-rooting-depths-database-for-gdes/

Thomas, B. F., Famiglietti, J. S., Landerer, F. W., Wiese, D. N., Molotch, N. P., & Argus, D. F. (2017). GRACE Groundwater Drought Index: Evaluation of California Central Valley groundwater drought. *Remote Sensing of Environment*, *198*, 384–392. https://doi.org/10.1016/j.rse.2017.06.026

United Water Conservation District. *Groundwater and Surface Water Conditions Report—2015* (Open-File Report No. 2017–01; p. 198). (2017). https://www.unitedwater.org/key-documents/#groundwater-conditions

U.S. Department of Agriculture (2012). National Agricultural Imagery Program. *Aerial imagery of the Santa Clara River watershed*. https://nrcs.app.box.com/v/naip/folder/17936490251.

U.S. Department of Agriculture (2021). The PLANTS database. National Plant Data Team, Greensboro, NC, USA. https://plants.sc.egov.usda.gov/java.

U.S. Drought Monitor (2021). *Time series for the Santa Clara River watershed*. https://droughtmonitor.unl.edu.

Van Loon, Anne F. (2015). Hydrological drought explained. *Wiley Interdisciplinary Reviews: Water*, *2*(4), 359–392. https://doi.org/10.1002/wat2.1085

Vicente-Serrano, S. M., Beguería, S., & López-Moreno, J. I. (2010). A Multiscalar Drought Index Sensitive to Global Warming: The Standardized Precipitation Evapotranspiration Index. *Journal of Climate*, *23*(7), 1696–1718. https://doi.org/10.1175/2009JCLI2909.1

Warter, M. M., Singer, M. B., Cuthbert, M. O., Roberts, D., Caylor, K. K., Sabathier, R., & Stella, J. (2020). *Onset and propagation of drought into soil moisture and vegetation responses during the 2012–2019 drought in Southern California* [Preprint]. https://doi.org/10.5194/hess-2020-479

Williams, A. P., Cook, E. R., Smerdon, J. E., Cook, B. I., Abatzoglou, J. T., Bolles, K., Baek, S. H., Badger, A. M., & Livneh, B. (2020). Large contribution from anthropogenic warming to an emerging North American megadrought. *Science*, *368*(6488), 314–318. https://doi.org/10.1126/science.aaz9600

Zhu, Z., Wulder, M. A., Roy, D. P., Woodcock, C. E., Hansen, M. C., Radeloff, V. C., Healey, S. P., Schaaf, C., Hostert, P., Strobl, P., Pekel, J.-F., Lymburner, L., Pahlevan, N., & Scambos, T. A. (2019). Benefits of the free and open Landsat data policy. *Remote Sensing of Environment*, *224*, 382–385. https://doi.org/10.1016/j.rse.2019.02.016

Zimmerman, R. C. (1969). *Plant Ecology of an Arid Basin: Tres Alamos-Redington Area, Southeastern Arizona.* (Geological Survey Professional Paper No. 485-D). U.S. Department of the Interior. https://pubs.usgs.gov/pp/0485d/report.pdf